**Trends Journal of Sciences Research**

# A Comparative Geophysical Study of the Sedimentary–Metamorphic Contacts in the Douala and Kribi–Campo Sub-Basins of Cameroon

**Njingti Nfor[1,2], Owona Angue Marie Louise Clotilde[1,2], Kue Petou Rokis Malquaire[2,3,5,*], Manguelle-Dicoum Eliezer[4], Lando Tsakou Julyo Achille[2], Piameu Kwagag Jöel[2]**

[1]Department of Physics, Advanced Teacher Training College, University of Yaoundé I, Yaoundé, Cameroon
[2]Postgraduate School of Sciences, Technologies & Geosciences, University of Yaoundé I, Yaoundé, Cameroon
[3]National Institute of Cartography, Yaoundé, Cameroon
[4]Department of Physics, University of Yaoundé I, Yaoundé, Cameroon
[5]School of Geosciences, China University of Petroleum, Qingdao, China
*Corresponding author: rokis.petou@yahoo.fr

**OPEN ACCESS**    **Research Article**

**Abstract** The magnetotelluric method has been used in this work to compare the nature of the sedimentary-metamorphic contacts of the Douala and Kribi-Campo sub-basins in Cameroon. The results show that the sedimentary-metamorphic contact zones for the two sub-basins, marked by a subsidence of the low resistivity materials on the sedimentary formations and uplift of the high resistivity materials characterized by intrusive bodies of higher values of resistivity on the metamorphic formations, are structurally similar,. However, the very low values of resistivity of rocks in the Douala sub-basin is suggestive of high porosity, permeability and high level of saline ions dissociation leading to high conductivity. These rocks should be of unconsolidated sediments for the sedimentary formation and gneiss for the metamorphic formation. On the contrary, the very high values of resistivity for rocks in the Kribi-Campo sub-basin indicate the absence of free mobile electrons and ions and low porosity, permeability and non-conductivity. The sedimentary formation of this sub-basin should be composed of limestone and conglomerates rocks with some gneissic and unconsolidated granitic materials. The rocks in the metamorphic formation should be completely granitic in nature. The shallow depth of penetration of only 4 km of telluric current in the Douala sub-basin is enough evidence that the tectonic events responsible for the emplacement of this contact zone were limited to the earth crust. On the other hand, in the Kribi-Campo sub-basin the tectonic events should have originated from within the earth mantle as the depth of penetration of telluric current attains 150 km.

*Keywords: Resistivity, Sedimentary, Metamorphic, Contact, Telluric, Tectonic*

# Introduction

The Douala/Kribi-Campo, Rio Muni, Gabon, Congo, Kwanza, Benguela, and Namibe basins of the onshore and offshore areas of Cameroon, Equatorial Guinea, Gabon, Republic of the Congo, Democratic Republic of the Congo, Angola and Namibia respectively, together form the Aptian salt, divergent passive margin basins of Equatorial West coast of Africa [1,2,3] These basins extend from Cameroon in the north with the Douala/Kribi-Campo basin to Namibia in the south with the Namibe basin (Figure 1). The basins share common structural and stratigraphic characteristics making them to be classified as Atlantic-type marginal sag basins that contain rocks ranging from Paleozoic to Holocene in age [4]. According to [1], the Aptian salt basins were formed during the breakup of the Gondwana super continent that led to the separation of North America, Africa and South America at the culmination of the Late Jurassic to Early Cretaceous rifting. The opening of the south Atlantic rift took place progressively from south to north from the Late Jurassic to the Lower Cretaceous [5] making the Douala/Kribi-Campo basin in Cameroon to be the youngest of the series. The basins have since undergone a complex history that can be divided into three stages of basin development: pre-rift stage (late Proterozoic to Late Jurassic), syn-rift stage (Late Jurassic to Early Cretaceous) and post-rift stage (Late Cretaceous to Holocene). The pre-rift stage incorporated several phases of intracratonic faulting and down warping during which continental clastic rocks of Carboniferous to Jurassic age were deposited in the Interior sub-basin. Aptian evaporites and clastic rocks in the west coastal basin areas provide evidence that rift-related sedimentation also occurred during the same time and could be the reason why most of these basins are essentially of sedimentary formation. Later basin wide normal faulting in these areas resulted in increased syn-tectonic, lacustrine sedimentation with the oldest syn-rift rocks consisting of Neocomian to Barremian fluvial including continental conglomerates and sandstones with lacustrine shales, limestones, and marls deposited in a broad, low-relief basin [6,7], which are unconformably overlying the Precambrian basement [1]. The pre-rift rocks in the offshore parts of the most of these basins consists of Pre-cambrian arkosic sandstones and conglomerates [8]. In Cameroon, two major episodes of tectonothermal deformation have been identified in the Ntem Complex which could have affected the emplacement of the Douala and Kribi-Campo sub-basins under study in this work. The first deformation episode is characterized by vertical foliation, stretching and vertical lineation and isoclinal folds, whose structural elements could mark the diapiric emplacement of the granitoids [9,10]. The second deformation episode is marked by the development of sinistral shear planes trending north–south to $N45^0E$, and partial melting of charnockitic and tonalitic members of the TTG suite and the greenstone belt country rocks, which [11] described as post-Archaean and post-charnockitic migmatisation. From data on metamorphic rocks from the Nyong series, this second event according to [12] could have occurred during the Eburnean orogeny.

The present work is aimed at comparing the nature of the sedimentary-metamorphic contacts of the Douala and Kribi-Campo sub-basins in Cameroon using results from magnetotelluric method of geophysical prospecting. The work is motivated by the fact that according to [3] the structural

systems of the Douala and Kribi-Campo sub-basins are similar to the Rio Muni basin in Equatorial Guinea but from [13] the two sub-basins still present quite remarkable differences in their litho-stratigraphic sequences. Again, according to [1] shelf-carbonates in the Kribi-Campo sub-basin are similar to the Rio Muni carbonate rocks to the southern-most part whereas in the Douala sub-basin to the northern-most part, the Mungo Formation lacks massive shelf-carbonate rocks. A knowledge of the type of sedimentation and the nature of contact from a geophysical view point could play an important role in revealing the reason for the similarities in structural systems and the differences in rock types between the Douala and Kribi-Campo sub-basins.



**Figure 1.** Map of the Aptian salt basins of equatorial west Africa showing the approximate locations of the Douala/Kribi-Campo, Rio Muni, Gabon, Congo, Kwanza, Benguela, and Namibe basins (modified from [1])

## Geological Settings

Geographically, the Douala and Kribi-Campo sub-basins are located in the Gulf of Guinea, at the northern end of the West African Atlantic ocean and cover a total area of $1.9 \times 10^4$ km [3] Both sub-basins lie to the southeast of the NNE-SSW trending Cameroon Volcanic Line, which forms their northern limit (Figure 1).

**Douala sub-basin**

The Douala sub-basin extends from latitude 3°20' N to 5°00' N and longitude 9° 00' E to 10°30' E. This sub-basin which is in the form of a triangle covers an estimated surface area of 7.0 x $10^3$ km² onshore [13] It is traversed by several fractured zones, amongst which are the Cameroon Fracture Zone (CFZ) and the Sanaga Fracture Zone (SFZ) which are known to have been reactivated several times in the past [13] It is bounded to the North and Northwest by the Cameroon Volcanic Line (CVL) whose limit with the Rio-Del-Rey basin is a superposition of this line on the NE-SW trending Central Africa Shear Zone (CASZ), which intersects the Atlantic Ocean in the northern end of the basin [13] To the southern portion it tapers towards Kribi where it is separated from the Kribi-Campo sub-basin by the Kribi Fracture Zone (KFZ). To the East of the basin is the Precambrian basement of the Pan African Mobile Belt. The sub-basin itself is lowlying with an average attitude of about 100 m above sea level, flat and swampy around the estuaries of the Wouri, Sanaga and Dibamba rivers which all empty into the Atlantic Ocean [14] Its surface is covered by coastal sands and blanketed with mangrove forest characteristic of sedimentary basins. The Douala sub-basin is characterized by igneous and metamorphic rocks constituting a Precambrian basement. Plutonic activity is shown by the presence of anatexites, granites and a charnockitic complex [15] Metamorphism is displayed by the presence of gneiss associated with migmatites in the eastern part of the sub-basin, amphibolites and micaceous quartzite sometimes with tourmaline in its northern and north-eastern fringes. This bedrock is affected by dextral shearing faults that are likely to be an extension of the transforming faults of Fernando Po and Ascension Fracture zones.[16]

The area under study is around the Dibamba River and forms part of the Loungahe series which is one of the four stratigraphic series that outcrop the edge of the Cameroon Atlantic coast [17,18,19]. It lies between latitude $4° \, 00' N$ and $4° \, 05' N$ and around longitude $10° \, 00' E$. The series consists of coarse unconsolidated sandstones mixed with marls, calcareous and silty clay whose age [17] gave as Senonian. The important fact about the series is that it marks the sedimentary-metamorphic contact between the sedimentary onshore Douala sub-basin and the Precambrian basement of the equatorial part of the Pan African Mobile Belt [15,20]

**Kribi-Campo sub-basin**

The Kribi-Campo sub-basin extends on the continental margin oriented NNE-SSW, between 2°10' - 3° 20'N and 9°-10°30' E [21] It covers a total area of about 6.2 x $10^3$ km² of which 45 km² is onshore. It is limited southwards by the Campo high, which separates both Kribi-Campo and Rio Muni basins. Its northern limit corresponds to the Kribi Fracture Zone (KFZ), which bounds the Douala sub-basin. The main faults in the region consist of the Kribi-Campo Fault (KCF) system which is also considered as a continuation of the Sanaga Fault Zone. This fault system is linked to the offshore portion of the KFZ fault system. The geological formations of Kribi-Campo basin belong to four major lithological and structural units [22] the Ntem Archean unit; the Nyong unit; the Neo-proterozoic cover and sedimentary formations. The rocks in this area are mainly schists, gneisses that have been intruded by granidiorites and sedimentary formations rocks such as limestones and sandstones [21,23] In the Kribi-Campo sub-basin, the transitional period is characterized by an evaporite unit [16] which has not been recognized in the Douala sub-basin.

The present study area is found at the south-western edge of the Ntem Complex and cuts across the southern portion of the Nyong and Ayina units and the south-western portion of the Ntem unit. The Nyong unit is made up of ancient Archean rocks of the Ntem basement that underwent Eburnean orogenesis. While the Ntem unit is dominated by massive and banded plutonic rocks of the charnockite suite and by intrusive tonalites, trondhjemites and granodiorites [10] The study area lies between latitude $2° 22'N$ and $2° 26'N$ and longitude $9° 57'E$ and $10° 41'E$, stretching from Campo to Nyabessan, having a minimum altitude of 39 m at Campo and maximum of 554 m around Nyabessan. It cuts across the sedimentary formation of the Kribi-Campo sub-basin and the metamorphic formation of the cratonic Ntem Complex.
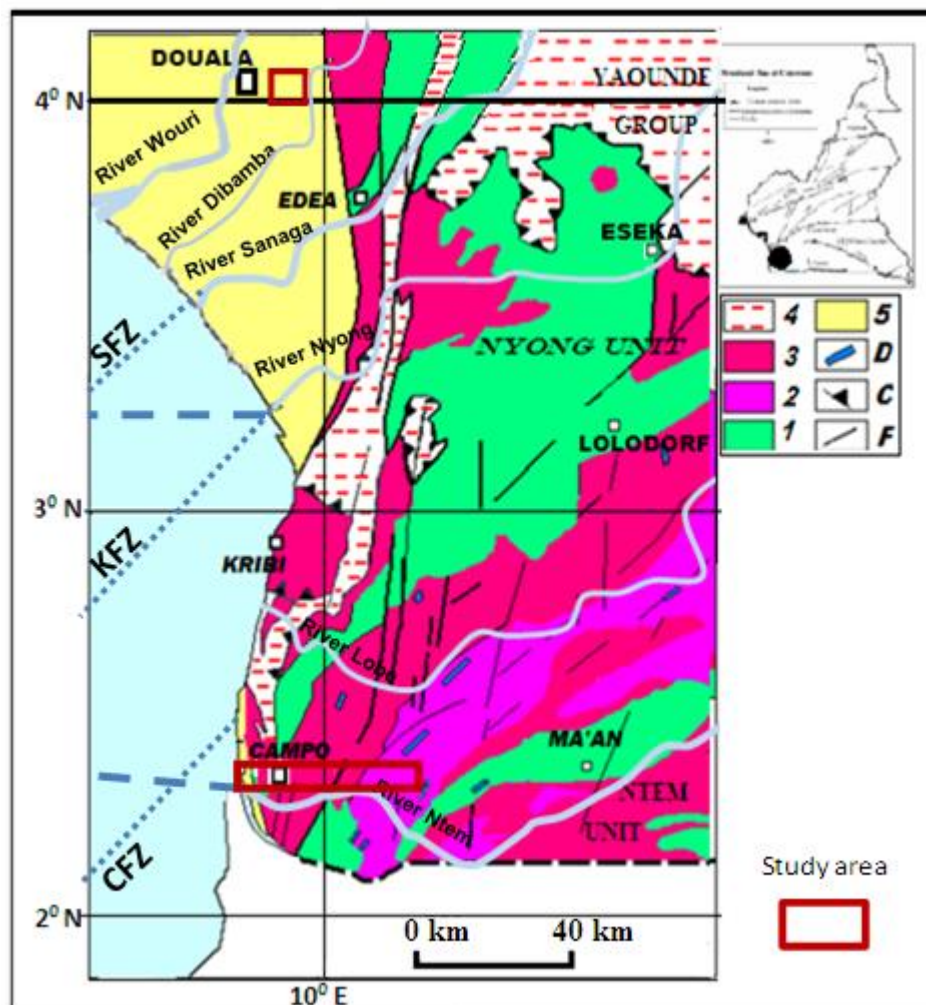


**Figure 2.** Structural Map showing the Douala and Kribi-Campo sub-basins of Cameroon (modified from [37] **1.** Archean and paleoproterozoic green rocks belts; **2.** Archean charnockites and granitoïds; **3.** Gneiss; **4.** Granitic mobile zone; **5.** Sedimentary basin; **C.** overlapping; **D.** Dolerites; **F.** Faults (SFZ: Sanaga Fault Zone; KFZ: Kribi Fault Zone; CFZ: Campo Fault Zone)

## Materials and Methods

### Magnetotelluric data

The magnetotelluric data used in this work were collected using an ECA 540 AMT resistivity meter [24] which has a frequency range from 4.1 Hz to 2300 Hz giving a total number of twelve frequencies. Field data is acquired at points called sounding stations which are chosen as a function of the existing

geographical features, knowledge and orientation of the subsurface geological features of interest such as faults and contacts that might have prompted the prospecting and accessibility. For each station a Global Positioning System (GPS) is first used to determine the angular coordinates and the altitude. Then, using the resistivity meter which is appropriately implanted, the method of rotation [25] is employed to determine the directions of polarization of the electric field (transverse electric; TE) and magnetic field (transverse magnetic; TM). For each station and in each of the polarization directions, twelve series of measurements at twelve different frequencies beginning from 2300 Hz to 4.1 Hz (frequency decreases with increasing depth) are made to get the component of electric field intensity, its mutually perpendicular component of magnetic field intensity and the values of the apparent resistivity. For each frequency and in each direction at least two resistivity values are acquired and the average calculated to get the apparent resistivity value. The data for each sounding station is made of position (altitude, longitude and latitude) and the frequency of alternating telluric current, components of electric and magnetic fields and apparent resistivity of subsurface rocks. Sounding stations grouped and aligned in a chosen direction constitute a profile. For each profile a particular sounding station is always chosen as base or control station with respect to which all other stations in the profile are referenced.

**Data for Douala sub-basin**

The difficulties faced in the collection of data for the Douala sub-basin were related to the inaccessible nature of the basin due to the mangrove forest and the fact that the frequency range of the ECA resistivity meter is considered too high for the telluric current to penetrate the deep-seated structures given the high conductivity of sedimentary rocks in this area. The principal directions were chosen in the North-South and East-West cardinal directions. Audiomagnetotelluric data were collected for 7 stations which have been grouped into two profiles. Profile Y is oriented from West to East with the base station at Mangoulle and profile D is oriented from South to North with a base station at Bonepoupa I. Each profile has a maximum of four stations. The directions were chosen both as a function of accessibility and with respect to the suspected zone of contact between the sedimentary and metamorphic formations which in this area is oriented SE and NW.

**Data for Kribi-Campo sub-basin**

The area of study is found in a dense equatorial forest into which access was difficult except for open fields and roads and also because of the presence of the Campo-Ma'an national park that covers a great portion of the area. Some of the identified geological and geographical features are the contact between the sedimentary Kribi-Campo sub-basin and cratonic Ntem Complex. The principal directions were chosen in the North-South and East-West cardinal directions. The audiomagnetotellurics data acquisition was conducted for 6 sounding stations along the main highways from Campo to Nyabessan. These sounding stations have been grouped to form two different profiles numbered $P_1$ *to* $P_2$ oriented NEE-SWW and W-E respectively with a maximum of four stations per profile. Both profiles have a common base station that is located in Campo at the edge of the the Kribi-Campo sub-basin. The two profiles are oriented to traverse the suspected contact between the sedimentary Kribi-Campo sub-basin and the metamorphic cratonic Ntem Complex.

**Processing and analysis of data**

**Apparent resistivity values**

From the two values of apparent resistivity that are got in the two principal directions in the field a geometric mean of apparent resistivity value ($\bar{\rho}$) is calculated using the formula:

$$\bar{\rho} = \sqrt{\rho_L \rho_T} \qquad (1)$$

Where $\rho_L$ and $\rho_T$ represent the longitudinal and transverse apparent resistivity values respectively, which are both measured in Ωm.

According to [26] no other physical property of naturally occurring rocks or soils displays such a wide range of values as the resistivity of rocks and minerals, extending from as low as $10^{-5} \Omega m$ to as high as $10^{15} \Omega m$ [14] In the upper part of the Earth's crust its value depends primarily on: the porosity, the permeability, the water content, the mobility, the concentration, the degree of dissociation of ions and on the chemical composition (salinity) of the water [27] From the information on the electrical resistivity of rocks provided by various authors amongst whom are: [26,26,27,29] and [14] the following factors are responsible for the wide variation:

*The presence of free mobile electrons and ions in the earth's subsurface:* The presence of clay, other weathered materials and high concentration of conductive minerals such as graphite, magnetite or pyrite in rocks lowers their resistivity.

*The existence of free ions in the ground water:* The dissociation of salts such as sodium chlorite and magnesium chloride leads to the presence of free ions, which may saturate ground water and lower the resistivity of rocks. Dry rocks and materials such as clean gravel or sand containing pure water even when water saturated, have high resistivity values.

*Permeability and porosity of saturated rocks and minerals:* The higher the permeability and porosity of rocks and minerals, the lower the resistivity values. Rock materials such as massive limestone, igneous and metamorphic rocks such as granite and basalt, which lack pore spaces have high resistivity values. This is equally true for rock materials such as dry sand or gravel, whose pore spaces lack water.

Apart from this variation which has to do with the rock composition and electrical conductivity, the resistivity of rocks and materials may be classified into three categories;

*Low resistivity ($\rho < 100\ \Omega m$):* Unconsolidated sediments and clay, marls and sand that is saturated with   saline water belong to this category.

*Medium resistivity* ($100\ \Omega m \leq \rho \leq 1k\Omega m$): Under this category are sand, marly sandstones and gravel saturated with fresh water.

*High resistivity (*$1\ k\Omega m > \rho \geq 10\ k\Omega m$*):* Massive limestone, igneous and metamorphic rocks such as granite and basalt belong to this third category.

**Pseudo depth of penetration of telluric currents**

The magnetotelluric method is based on the principle of the skin-effect [30] According to this principle, the depth to which an electromagnetic wave penetrates into the earth subsurface depends on the frequency at which it impinges on the surface. When the frequency is very high the telluric

current remains on a thin subsurface of the earth, called the pseudo-depth of penetration given by the Cagniard equation for magnetotelluric prospecting as:

$$P = 0.503 \sqrt{\rho T} \tag{2}$$

Where $T$ is period measured in seconds ($s$), which is the reciprocal of frequency.

For each station and as a function of the frequency and geometric mean apparent resistivity value, the pseudo depth of penetration of the telluric current is determined.

**Iso-resistivity contour maps**

An iso-resistivity is a plot of the values of geometric mean apparent resistivity values which has the logarithm of the frequency of electromagnetic waves in descending order with increasing pseudo-depth on the vertical axis against the distance from a base station taken as origin on the horizontal axis. This plot gives a series of contour lines that represent the paths connecting points with the same geometric mean apparent resistivity values. These contour lines provide a two-dimensional representation of the variation of apparent resistivity with depth for vertical cross-section through a slice of earth under consideration. They illustrate the shape of the structures within the sub-surface. According to [31] when the subsurface is homogeneous and has uniformly varying apparent resistivity values, the contours are horizontal and parallel, uniformly spaced and unfolded. Abrupt changes in the values of apparent resistivity are indicated on the contour map by curved contour lines. These might be as results of folds, faults, fractures or intrusions. Contour lines that are in faulted areas are sub-vertical or vertical and closely packed along the line of high gradient.

**Geo-electric sections**

A geo-electric section is a 2D presentation of the earth's subsurface that is described by two fundamental parameters: the resistivity of the subsoil $\rho_i$ and thickness of depth $h_i$ [14] The geo-electric section can also be described as a function of other parameters such as conductance, resistance and coefficient of anisotropy. It is thus employed to show how the electrical properties of rocks and rock materials can be averaged over a large volume of earth, which may not necessarily be homogeneous [14] For a layered sequence of rocks, the geo-electric section shows boundaries between layers represented by pronounced resistivity contrasts. In the geo-electric section, it is possible to recognize structures like folds, faults and intrusions. A fault is recognized in a geo-electric section by a break in the continuity of the normal geo-electric sectional sequence [14] Some amount of geo-electric section is always repeated or missing at the fault contact [31] From the geo-electric section, a measure of the fault magnitude is equal to the thickness of the missing or repeated section [32]

A geo-electric section differs from a geologic section when the boundaries between geologic layers do not coincide with the boundaries between layers characterized by different resistivity values. This is because, the electric boundaries separating layers of different resistivity values may or may not coincide with boundaries separating layers of different geologic age or different lithological composition. In some cases several geo-electric layers may be distinguished within a lithologically homogeneous rock. The reverse can also occur when layers of different lithology or ages, or both, have the same resistivity and thus form a single geo-electric layer [27]

# Results and Interpretation

The results presented in this section for the two sub-basins consist of iso-resistivity maps and geo-electric sections. The iso-resistivity maps have been obtained from the geometric mean apparent resistivity values using the MT2DInvMatlab computer program [33]. This is a two-dimensional modeling program for magneto-telluric data which works through a combination of two interactive algorithms in FORTRAN and MATLAB. MT2DInvMatlab employs the finite element method to calculate magneto-telluric 2-D responses with an incorporated smoothness-constraint least-square inversion method. The geoelectric sections are generated directly by the same program from the iso-resistivity contour maps.

**Results from the Douala sub-basin**

**Iso-resistivity contour maps**

The iso-resistivity contour maps for the Douala sub-basin around the sedimentary-metamorphic contact have been drawn for two profiles: the contour map of profile $D_1$ as shown in Figure 3a is West-East oriented and has a length of about 7 km while that of profile $D_2$ as shown in Figure 3b is South-North oriented and has a length of about 12 km.

For the purpose of interpretation and following the shape depicted in the maps, the colour codes vary from deep blue to grey for resistivity values ranging from $0 \, \Omega m \leq \rho \leq 3 \, \Omega m$, from deep green to deep yellow for resistivity values ranging from $3 \, \Omega m < \rho \leq 18.0 \, \Omega m$ and from orange to purple for resistivity values ranging from $18 \, \Omega m < \rho \leq 316 \, \Omega m$. It can be seen that $316 \, \Omega m$ is the highest value of resistivity acquired for the most resistive rocks in this area of study.

Rock materials with the first range of resistivity values occupy the western and Southern portions of the Figure 3a and Figure 3b up to lateral distances of 4 km and 8 km respectively and from the surface to varied depths. These may correspond to sedimentary rocks of the Douala sub-basin in this area. The second range of resistivity values occupy a lateral distance of about 1 km in Figure 3a and 500 m for Figure 3b and from the surface it extend to depths of 400 m and beyond 700 m respectively. This may correspond to a transitional mixture of sedimentary and metamorphic materials still undergoing transformation through contact metamorphism. The third range of resistivity values extends from a lateral distance of 2 km for both Figure 3a and Figure 3b and from the surface to the full pseudo-depth of telluric current which is about 4 km in this area. What is most remarkable here is the highly distinct nature of an intrusive body represented by the predominantly purple colour code with a maximum resistivity of $316 \, \Omega m$. This material seems to have come directly from underneath at depth beyond 4 km. As shown in Figure 3a, this material is found on the surface around the area of transition between the sedimentary and metamorphic formations.
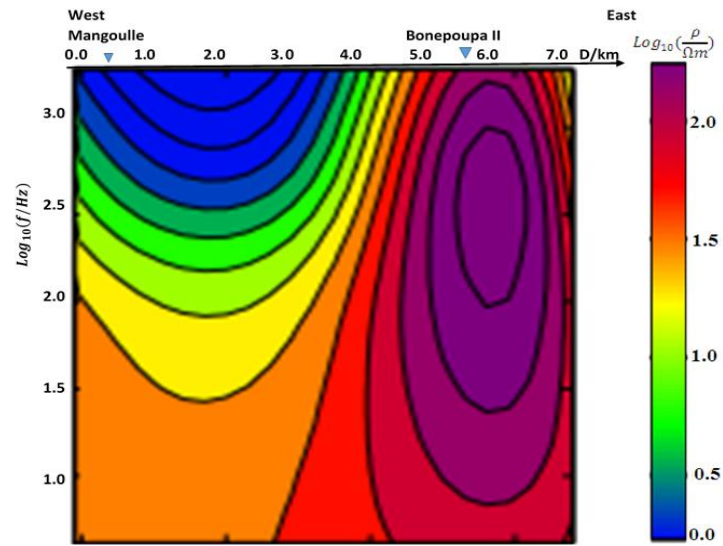
**Figure 3a.** Iso-resistivity contour map $D_1$ oriented from West to East
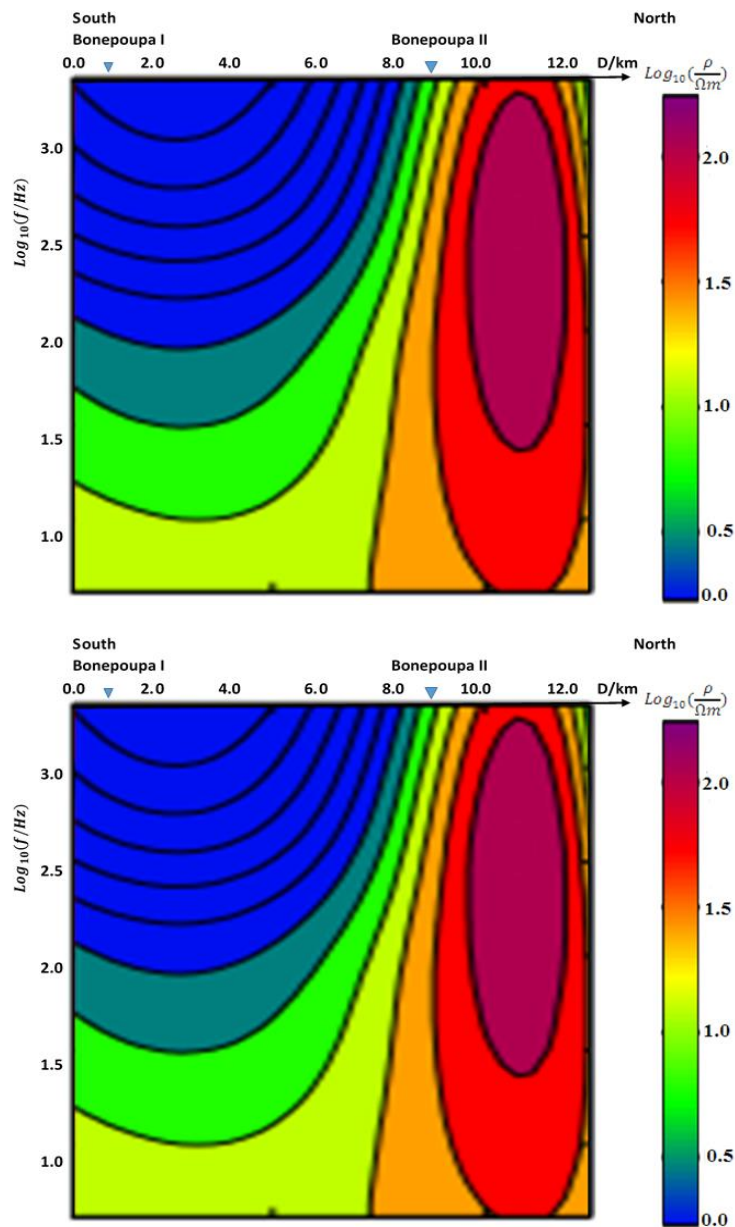


**Figure 3b.** Iso-resistivity contour map Y West - East orientation

The conclusion can be drawn that the western and southern portions of the Figure 3a and Figure 3b respectively are the sedimentary formation while the metamorphic formation is to the east and north of the zone. The iso-resistivity contour lines in the sedimentary formation are sparsely distributed but very closely packed in the zone of contact with the metamorphic formation. A zone of transverse compression and contraction of contour lines resulting to synclinal and anticlinal features mark the transition from the sedimentary to the metamorphic. This is a zone of transitional or contact metamorphism. The synclinal structure which seems to have been caused by the weight of the overlying beds on the substratum due relatively strong gravity gliding force and differential compaction of the sediments is more pronounced near the surface and close to the area of compaction of the sediments. The anticlinal contour lines on the metamorphic portion indicate a highly compressive zone probably resulting from the action of a very strong radially directed force that led to upwelling of relatively high resistivity material from a depth beyond 4 km to the near surface. The contour lines in the area are practically vertical on both sides of the dyke-like intrusive body and might have been caused by an abrupt lateral resistivity change. This shows that the resistivity of the substratum rocks most be higher compared to that of the overlying layers. The metamorphic formation presents multilayered sub-vertical units with the relatively high resistivity material plunging deep under the sedimentary formation at depths beyond 4 km on the western and southern ends of both Figure 3a and Figure 3b. This shows an extension of the metamorphic formation under the sedimentary formation of the sub-basin at depth.

**Geoelectric sections for Douala**

Figure 4 and Figure 4b give a presentation of the geoelectric sections for the two profiles in Douala sub-basin with respect to three parameters: the lateral spread of the stations from the base stations, the pseudo-depth of penetration of the electromagnetic waves and the geometric mean values of apparent resistivity. There are two base stations: one to the west of profile Y at Mangoulle and the other to the south of profile D at Boneppoupa I.

A general observation of the two geoelectric sections reveals that: the material of low resistivity0 $\Omega m$ to 3 $\Omega m$) of blue to arch grey colour code, representing the sedimentary formation is highly distinct and is found to the west of Figure 4a where it extends from the base station to about 3 km toward the east and from the surface down to a depth beyond 4 km. In Figure 4b, material with this same resistivity range extends from the base station in the south to about 6 km towards the north and from the surface down to a depth beyond 4 km. The transitional or contact metamorphic material of green to yellow colour code and resistivity range3 $\Omega m < \rho \leq 18 \ \Omega m$, is found in Figure 4a between 3 km and 4 km of lateral distance from the base station and from the surface down to a depth of 2 km and from a lateral distance between 4 km and 5 km at a depth of from 2 km to beyond 4 km. The emplacement of this material seems to have constituted a dyke-like fault zone of magnitude greater than 4 km from the surface to deeper depths. In Figure 4b, the transitional material is found at varied depths and stretching over varied lateral distances. At depths from 2 km, it is found sandwiched at different point between the materials of sedimentary formation. At a lateral distance of from 6 km to 10 km from the origin, it seems to constitute a dyke-like structure of 2 km magnitude from the surface. The portion occupy by the complete metamorphic materials of colour

from orange to purple and resistivity range $18 \ \Omega m \ < \rho \leq \ 316 \ \Omega m$ is very distinct. For Figure 4a these materials extend from a lateral distance of from 4 km to above 7 km, with a depth range greater than 4 km from the surface. In Figure 4b the same material is found at a depth of 2 km from the surface where it extends over a lateral distance of from 6 km to 10 km from the origin and from 10 km to over 12 km on the surface and with a depth range greater than 4 km from the surface. The intrusive high resistivity ($316 \ \Omega m$) purple colour code material has its roof at a depth of 1 km and bottom at 2 km over a lateral distance of 5 km to 6 km in Figure 4a and at a depth of between 2 km to above 3 km over a lateral distance of 10 km to above 12 km in Figure 4b.

Overall, due to the limitations impose by the equipment, data could not be collected for depths beyond 4 km and the information presented here seems to be limited to the upper part of the earth crust only.
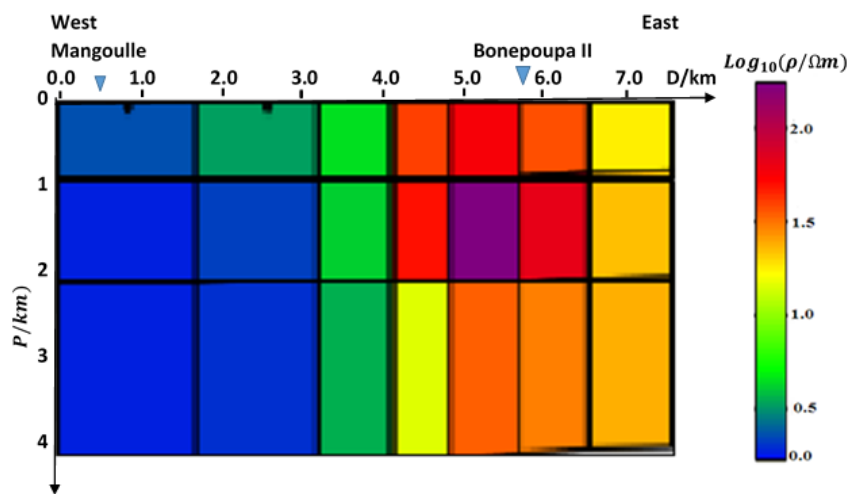


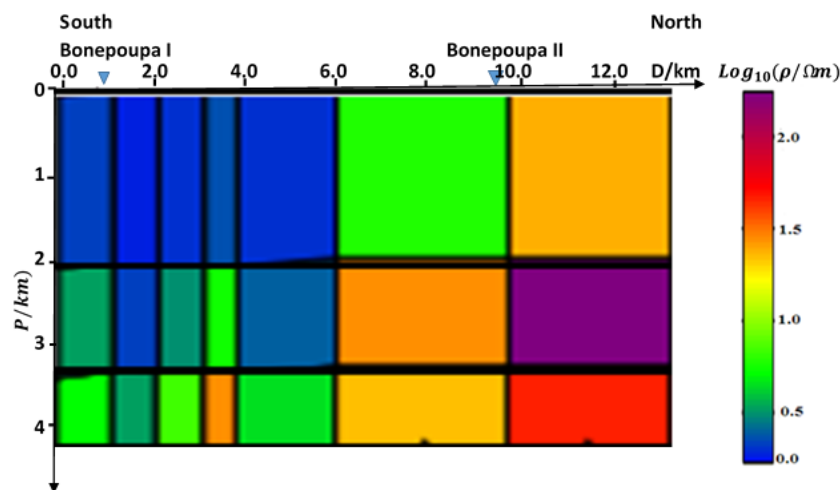**Figure 4a.** Iso-resistivity contour map Y West - East orientation



**Figure 4b.** Iso-resistivity contour map Y West - East orientation

## Results from Kribi-Campo sub-basin

### Iso-resistivity contour maps

The iso-resistivity contour maps for the Kribi-Campo sub-basin around the sedimentary-metamorphic contact have been drawn for two profiles: the contour map of profile $P_1$ as shown in

Figure 5a is Southwest west - Northeast east oriented and has an approximate length of 60 km while that of profile P₂ as shown in Figure 5b is West-East oriented and has a length of about 70 km.
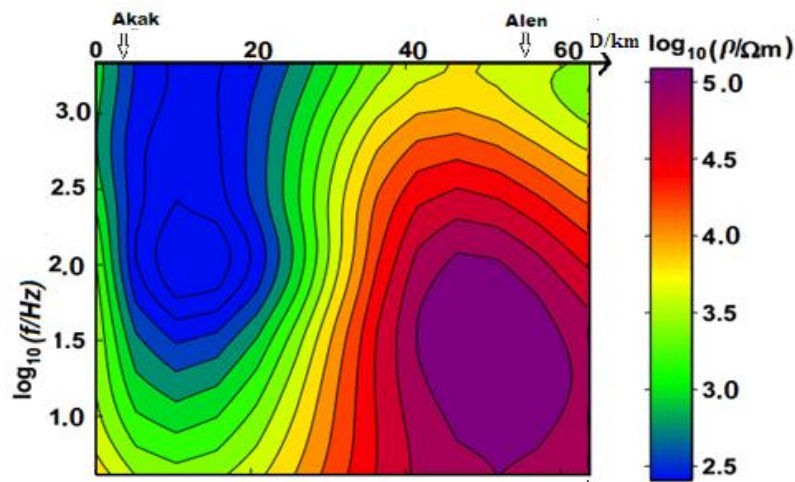


**Figure 5a.** Iso-resistivity contour map P₁ oriented SWW-NEE
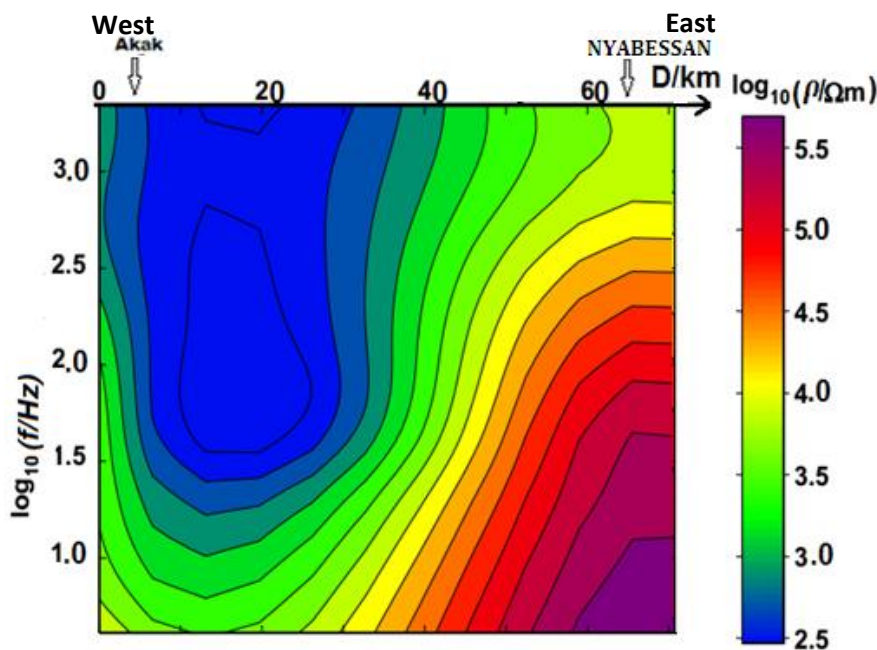


**Figure 5b.** Iso-resistivity contour map P₁ oriented West-East

The colour codes in the Figure 5a and Figure 5b above vary from deep to light blue for resistivity values ranging from 316 *Ωm to* 1 *kΩm,* from deep green to deep yellow for resistivity values ranging from 1 *kΩm  to* 10 *kΩm*  and finally from orange through red to deep purple for resistivity values ranging from 10 *kΩm  to* $5 \times 10^4$ *kΩm.* Rock materials with the first range of resistivity values start from the western ends of both figures and extend for over 30 km laterally and from the surface to a maximum depth of about 2 km. These may correspond either to rocks of the sedimentary Kribi-Campo sub-basin or weathered and unconsolidated metamorphic materials [23，34，35] of the cratonic Ntem Complex. The second range of resistivity values starts from about 30 km from the base station and extend throughout, seemingly covering the rest of the lateral distance and from the surface to depths above 28 km. This may correspond to sedimentary and weathered metamorphic

materials that have been completely (re-)transformed into metamorphic rocks through the process of contact metamorphism. The third range of resistivity values equally starts from about 30 km from the base station and extend laterally over the entire area and from a minimum depth of 5 km to above 90 km. These may correspond to metamorphic rocks of plutonic origin which forms the Precambrian basement of the cratonic Ntem Complex. They might mostly be made up of massive and banded plutonic rocks of the charnockite suite and by intrusive igneous, granite and granodiorites rocks [10]

The general nature of the contour lines in the Figure 5a and Figure 5b, is such that they are either closed or open. The closed contour lines are around the 316 $\Omega m$ to 1 $k\Omega m$, 1 $k\Omega m$ to 10 $k\Omega m$ and the 10 $k\Omega m$ to $5 \times 10^4$ $k\Omega m$ resistivity values. They are concentric contour lines that are either circular or ellipsoidal in shape. The closed contours around the 316 $\Omega m$ to 1 $k\Omega m$, resistivity values represent sedimentary materials from the near-surface of the earth that might have undergone subsidence due probably to the weight of overburden and petro-static pressure. The closed contours around the 10 $k\Omega m$ to $5 \times 10^4$ $k\Omega m$ resistivity values represent plutonic materials of Precambrian origin that might have welled up from underneath due probably to some upward vertical magmatic forces and which became cut off from the substratum and lodged in the architectural structure of the relatively low resistivity materials. This intrusive material is found at a pseudo-depth range of between 15 km to 90 km in Figure 5a. Around the zone of probable contact between the sedimentary Kribi-Campo sub-basin and the metamorphic cratonic Ntem Complex, the materials of resistivity range of values from 1 $k\Omega m$ to 10 $k\Omega m$ are sandwiched between the two formations of low and very high resistivity and also extend from the surface down to the basement. It can be said that the zones of sandwich correspond to fault systems, which are either vertical or sub-vertical in nature. The sub-vertical or completely vertical and parallel contour lines indicate violent tectonic forces that resulted to either fractures or faults. The open contour lines that start from the bottom of the map show that the material welled up from the subsurface at some depth that the telluric current could not reach and might therefore represent the substratum rocks which is Precambrian in nature. This is the case with the two figures. The wavy nature of the iso-resistivity contour lines indicate that apart from the subductive forces of the overburden sedimentary materials and upwelling forces of the magmatic materials, there also existed laterally directed compressional tectonic forces. These led to low resistivity materials sinking from above to form synclinal folds and high resistivity material rising from below to form anticlinal folds. These highly compressed and deformed nature of the iso-resistivity contour lines is also suggestive of the violent nature of the tectonic forces that must have been at the origin of the emplacement of the rocks in this region.

Overall, the values of the resistivity are generally high showing that the material occupying a large portion of the area of study is highly consolidated and can be considered to be globally metamorphic.

**Geoelectric sections for Kribi-Campo**

Figure 6a and Figure 6b give a presentation of the geoelectric sections for the two profiles in Kribi-Campo sub-basin with respect to three parameters: the lateral spread of the stations from the base station, the pseudo-depth of penetration of the electromagnetic waves and the geometric mean values of apparent resistivity.

A general observation of all the geoelectric sections reveals that: the low resistivity material (316 *Ωm to* 1 *kΩm*) of blue colour code, representing the sedimentary material, is only found at near surface, up to about 2 km depth from the western extreme of both figures up to about 20 km laterally. It disappears completely beyond this depth and length giving room for the moderately high resistivity material (1 *kΩm to* 10 *kΩm* ) of arch-grey colour code, which extends to further depth of about 12 km. This represents the area covered by the sedimentary Kribi-Campo sub-basin at this zone of contact of metamorphic cratonic Ntem Complex. The remaining portions of the geoelectric sections extending laterally over 60 km and to depth of over 150 km in the two figures is covered by the very high resistivity material ($\rho > 10$ *kΩm*) of colour code from green to purple. The figures show that the very high resistivity material did not originate from the earth crust only (average 35 km below the earth surface) but as far below the earth surface as the mantle.
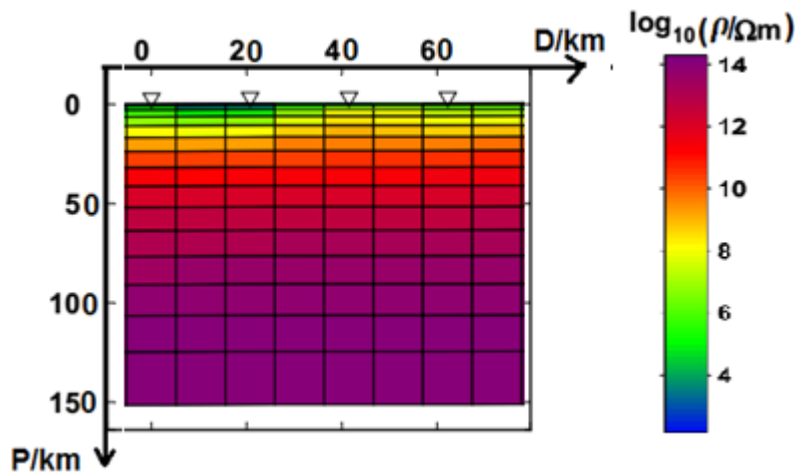


**Figure 6a.** Geoelectric section for Southwest west – Northeast east orientation
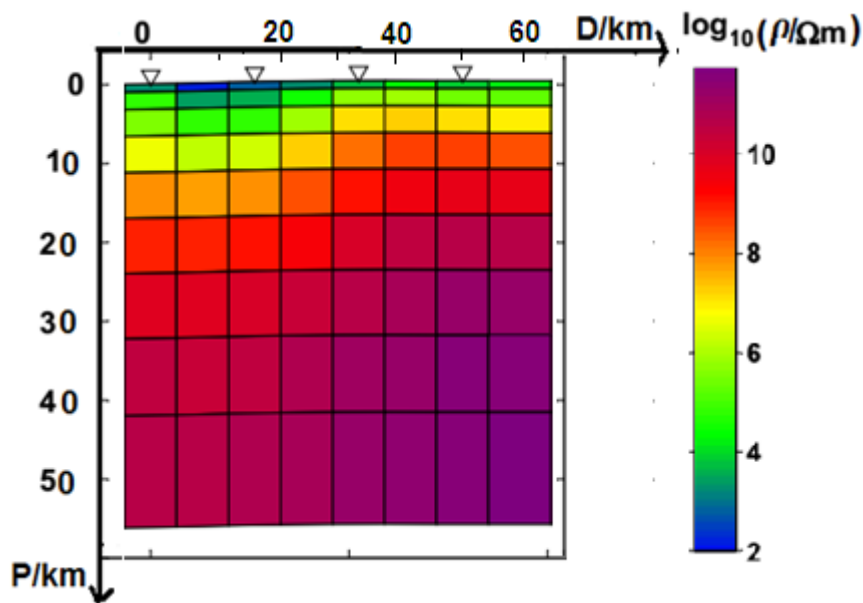


**Figure 6b.** Geoelectric section for West – East orientation

## Comparative Discussion

The values of resistivity of rocks in the Douala sub-basin range from $0\ \Omega m$ to a maximum of $316\ \Omega m$) and fall within the low and medium resistivity categories respectively. These show the probable presence of unconsolidated sediments, clay, weathered materials, high concentration of conductive minerals and free ions derived from saturated saline solutions for the low resistivity materials and sand, marly sandstones and gravel saturated with fresh water for the medium resistivity materials. It also indicates the high permeability and porosity of the rocks. The sedimentary formation may be considered to be made up of unconsolidated sediments, clay, marls and sand, saturated with saline water. The low values of resistivity for the metamorphic formation around the contact zone (maximum of $18\ \Omega m$) show that the materials were probably derived from the contact metamorphism of sediments and pre-existing igneous rocks under intense heat and pressure. The approximately parallel nature of the contour lines around this area indicates that through some sort of thermal, physical and/or chemical processes the final gneiss rocks formed at contact should be foliated and composed of layers of sheet-like planar structures like slates. The material in the Pan African Mobile Belt portion of the metamorphic formation should be predominantly composed of gneiss rock. The geoelectric sections in 4a and 4b show a maximum depth of 4 km attained by the telluric current in both the sedimentary and metamorphic formations, indicating that most of the tectonic events that led to the formation of the Douala sedimentary sub-basin were at near surface and probably limited within the earth crust.

Contrary to what is obtained in the Douala sub-basin around the study area, the rocks of the Kribi-Campo sub-basin at its area of study have very high resistivity values ranging $316\ \Omega m$ to $5 \times 10^4\ k\Omega m$. These values lie within the medium and high resistivity categories, which indicate the presence of sand, marly sandstones and gravel saturated with fresh water on the one hand and massive limestone, igneous and metamorphic rocks such as granite on the other. It also shows that in terms of composition, the subsurface rocks within the area of study lack free mobile electrons and ions and are also non-porous, non-permeable and highly non-conductive. From the comparatively high values of resistivity for the sedimentary formation of this sub-basin the sediments there are made up not only of arkosic sandstones interbedded with shales, limestone and conglomerates [36] but should also have some gneissic and unconsolidated granitic materials. This formation is limited within a depth of about 2 km around Campo. At the zone of contact between the sedimentary and metamorphic formations, the metamorphosed materials should have been formed under some sort of intense heat and pressure leading to a "granite-gneiss" rock type. This transformation should be more of structural than mineralogical as the geoelectric sections in Figure 6a and Figure 6b do not show any clear evidence of abrupt changes. The comparatively exceedingly high values of resistivity (about $5 \times 10^4\ k\Omega m$) of the metamorphic cratonic Ntem Complex portion of the study area and it extent in depth (going down to beyond 150 km) as shown in the geoelectric sections of Figure 6 suggests that the tectonic events that led to the emplacement of the granites in this area originated from within the earth's mantle. Surface gneiss rocks found in the area seem to have been formed through a process of regional metamorphism from pre-existing igneous and sedimentary rocks.

# Conclusion

This work was aimed at employing the geophysical magnetotelluric method to compare the nature of the sedimentary-metamorphic contacts of the Douala and Kribi-Campo sub-basins in Cameroon, which from most literature are considered as a single basin with the Kribi-Campo sub-basin to the south being an outcrop of the Douala sub-basin to the north. Although the two sub-basins have similar structural systems they are said to still present quite remarkable differences in their litho-stratigraphic sequences. The conclusions of this work are that:

Structurally, the contact zones for the two sub-basins are similar, given that they are marked by a subsidence of the low resistivity materials on the sedimentary formations and uplift of the high resistivity materials characterized by intrusive bodies of higher values of resistivity on the metamorphic formations.

The very low resistivity values of rocks in the Douala sub-basin is suggestive of high porosity, high permeability and high level of saline ions dissociation. These rocks should be of unconsolidated sediments, clay, marls and sand for the sedimentary formation; sheet-like planar foliated gneiss rocks around the contact area and complete gneiss on the metamorphic formation of Pan African Mobile Belt. On the contrary, the very high values of resistivity for rocks in the Kribi-Campo sub-basin is indicative of the fact that they lack free mobile electrons and ions and are non-porous, non-permeable and highly non-conductive. Apart from being composed of limestone and conglomerates the rocks in the sedimentary formation of this sub-basin should also have some gneissic and unconsolidated granitic materials. At contact the rocks should be of granite-gneiss type and on the metamorphic formation of cratonic Ntem Complex the rocks should be completely granitic. This transition is more structural than mineralogical.

The shallow depth of penetration of only 4 km of the telluric current in both the sedimentary and metamorphic formations in the Douala sub-basin as depicted in the structural geoelectric presentations gives concrete evidence that the tectonic events responsible for the emplacement of the contact zone were limited to the earth crust. On the other hand, in the Kribi-Campo sub-basin there is enough evidence that the tectonic events came from within the earth mantle as deep down as 150 km below the earth surface.

These conclusions are a major contribution to the geology and geophysics about the two sub-basins and may help in redirecting future research works in both areas.

# Acknowledgements

# References

[1]     Brownfield Michael, E., and Charpentier Ronald R. (2006). Geology and Total Petroleum Systems of the West-Central Coastal Province (7203), West Africa. U.S. Geological Survey Bulletin 2207-B, Reston, Virginia: 2006

[2]     Edwards, Alan, and Bignell Roger, (1988). Hydrocarbon potential of W. African salt basin: Oil and Gas Journal, v. 86, no. 50,71–74.

[3]     SNH, (2015). Blocks on offer in the Rio Del Rey, Douala/Kribi-Campo and Mamfe basins. http://www.snh.cm

[4]     Clifford, A. C. (1986). African oil—past, present, and future, in Halbouty, M.T., ed., Future petroleum provinces of the world: American Association of Petroleum Geologists Memoir 40, 339–372.

[5]     Rabinowitz, P. D., Labrecque, J. (1979). The Mesozoic South Atlantic Ocean and evolution of its continental margins. J Geophys Res 1979; 84 (11): 5973-6002.

[6]     Ross, D. (1993). Geology and hydrocarbon potential of Rio Muni area, Equatorial Guinea: Oil and Gas Journal, v. 91, August 23, 1993, 96–100.

[7]     Turner, J. P., (1995). Gravity-driven structures and rift basin evolution—Rio Muni Basin, offshore West Africa: American Association of Petroleum Geologists Bulletin, v. 79, no. 8, p. 1138–1158.

[8]     Nguene, F. R, Tamfu, S. F., Loule, J. P., Ngassa, C. (1991). Palaeoenvironments of the Douala and Kribi/Campo sub-basins, in Cameroon, West Africa. In: Curnelle R, Ed. African Geology, 1 st Colloquium on Stratigraphy and Paleogeography of West African Sedimentary Basins, 2 nd Colloquium of African Micropaleontology. Libreville 1991, Boussens: Elf Aquitaine 1992; 129-39.

[9]     Shang, C. K. (2001). Geology, Geochemistry and Geochronology of Archaean Rocks from the Sangmelima Region, Ntem complex, NW Congo craton, South Cameroon. Ph.D. Thesis, University of Tu¨bingen, Germany, 313p.

[10]    Tchameni, R., Mezger, K., Nsifa, N.E., Pouclet, A., (2001). Crustal origin of Early Proterozoic syenites in the Congo craton (Ntem complex), South Cameroon. Lithos 57, 23–42.

[11]    Nsifa, E.N., Riou, R., (1990): Post Archaean migmatization in the charnockitic series of the Ntem complex, Congo craton, southern Cameroun. 15th Colloquium on African Geology, Publications Occasionnelle, CIFEG 22, 33–36.

[12]    Lasserre, M., Soba, D., (1976). Age Libérien des granodiorites et des gneiss a pyroxènes du Cameroun Méridional. Bulletin BRGM 2 (4), 17–32.

[13]    Njoh O. A., Essien J. A., et Tembi A., (2014). Albian – Turonian palynomorphs from the Mundeck and Logbajeck Formations, Ediki River, north-western part of Douala sub-basin. Sciences, Technologies et Developpement, volume 15, 66 – 77, ISSN 1029 – 2225

[14]    Njingti-Nfor (2004). New Methods of Analysing and Interpreting Audiomagnetotellurics Data. Doctorate thesis, University of Yaoundé I, Yaoundé, 185 p.

[15]    Recard N. N. P., Mfayakouo C. B., and Bitom D., (2014). Paleogeographic Evolution of the Eastern Edge of the Douala Basin from Early Cenomanian to Turonian. The Open Geology Journal, 8, 124-141.

[16]    Meyers J. B., Rosendahl B. R., Groschel-Becker H., Austin Jr J. A., Rona P. A. (1996). Deep penetrating MCS imaging of the rift-to-drift transition, offshore Douala and North Gabon basins, West Africa. Mar Petrol Geol 1996; 13 (7): 791-835.

[17]    De Vries, (1936). Mission de recherche des hydrocarbures du Cameroun effectué en 1935 – 1936. Rapport général, Services des mines au Cameroun. 72p.

[18]    Njike Ngaha P., R, (2004). Palyno-stratigraphique et reconstitution des paleoenvironnements du Crétacé de l'Est du Bassin sédimentaire de Douala (Cameroun).

[19]    Njike, N. P. R., and Belinga, S. M., (1987). Le Diachronisme du grès de base, le paléooenvironnement et le rôle de l'ouverture de l'Atlantique Sud. Ann. Fac. Sci. Terre IV No. 3-4, 103 – 119.

[20]    Dumort, J. C., (1968). Notice explicative sur la faille de Douala – Ouest. Direction des mines et de la géologie du Cameroun. 69p. index, 1 carte h.t.

[21]    Djomeni A. L., Ntamak-Nida M. J., Mvondo F. O., Kwetche P. G. F., Kissaaka J. B. I., and Mooh-Enougui E. (2011). Soft-sediment deformation structures in Mid-Cretaceous to Mid-Tertiary deposits, Centre East of the Douala sub-basin, Cameroon: Preliminary results of the tectonic control. Syllabus Review 2 (3), 2011: 92 - 105

[22]  Maurizot, P., Abessolo, A., Feybesse, J. L., Johan, V. and Lecomte, P. (1986). Etude et prospection minière du sud-ouest Cameroun. Synthèse des travaux de 1978 à 1985. Rapport, BRGM, 274p

[23]  Toteu, S. F., Penaye, J., Poudjom Djomani, Y. H., (2004). Geodynamic evolution of the Pan-African belt in Central Africa with special reference to Cameroon. Canadian Journal of Earth Sciences, 41, 73–85.

[24]  Benderitter, Y. (1982). Interprétation des mesures magnétotelluriques obtenues avec un résistivimètre ECA. CNRS, CRG, Garchy.

[25]  Manguelle-Dicoum, E. (1988). Etude Géophysique des structures superficielles  et profondes de la région de Mbalmayo. Thése de Doctorat es-sciences (Géophysique). Université de Yaoundé, 202 p.

[26]  Parasnis D. S. (1979). Principles of Applied Geophysics. Chapman and Hall. (3rd Edition) London, 275p.

[27]  Zohdy, A. A. R., Eaton, G. P. and Mabey, D. R. (1990). Application of Surface Geophysics to Ground-Water Investigations. 4th Edition, United States Geological Survey, Denver, 123p.

[28]  Geza K. (1966). Principles of Direct Current Resistivity Prospecting. Geopublication Associates Series 1- No. 1

[29]  Telford, W. M., Geldart, L. P., Sheriff, R. E. and Keys, D. A. (1990). Applied Geophysics. Cambridge University Press, Cambridge. https://doi.org/10.1017/CBO9781139167932

[30]  Cagniard, L. (1953). Basic Theory of the Magnetotelluric Method of Geophysical Prospecting. Geophysics, 18, 605-635. https://doi.org/10.1190/1.1437915

[31]  Redmond, J. L. (1972). Null Combination in Fault Interpretation. Bulletin —American Association of Petroleum Geologists, 56, 150-166.

[32]  Bates, R. L. and Jackson, J. A. (1987). Glossary of Geology. 3rd Edition, American Geological Institute, Alexandria, 788 p.

[33]  Lee, S. K., Kim, H. G., Song, Y. and Lee, C. (2009). MT2DInvMATLAB—A Program in FORTRAN and MATLAB for 2D Inversion. Computer and Geoscience, 35, 1722-1734.

[34]  Njingti-Nfor, Manguelle-Diccoum, E., Mbom-Abane and Tadjou, J. M. (2001). Evidence of Major Tectonic Dislocations along the Southern Edge of the Pan African Mobile Belt and the Congo Craton Contact in the Southern Region of Cameroon. The 2nd International Conference on the Geology of Africa, Assuit, Vol. 1, 799-811.

[35]  Owona Angue, M. L. C., Nguiya, S., Nouayou, R., Tokam Kamga, A. P. and Manguelle-Dicoum, E., (2011). Geophysical Investigation of the Transition Zone between the Congo Craton and the Kribi-Campo Sedimentary Basin (South-West Cameroon). South African Journal of Geology, 114, 145-158.

[36]  Iboum Kissaaka, J. B., Ntamak-Nida, M. J., Ngueutchoua, G., Mvondo Owono, F., Djomeni Nitcheu, A. L., Fowe Kuetche, P. G. and Bourquin, S. (2016). Syn-rift Tectonic Markers from Outcrops and Offshore Seismic Data of the Southern  Part  of Kribi-Campo Sub-Basin (Cameroon, West African Margin). Comunicações Geological, 99, 35-42.

[37]  Kue Petou R. M., Owona Angue. M. L. C., Njingti-Nfor, N., Ndougsa-Mbarga, T. and Manguelle-Dicoum, E. (2017b). Determination of Structural and Geometrical Parameters of the Kribi-Campo Sedimentary Sub Basin Using Gravity Data. International Journal of Geosciences, 8, 1210-1224. https://doi.org/10.4236/ijg.2017.89069